# Appearance of High-Dynamic Range Images in a Uniform Lightness Space

*John J. McCann and Alessandro Rizzi; McCann Imaging, Belmont, MA 02478, USA and Dipartimento di Tecnologie dell'Informazione, Università degli Studi di Milano, 26013 Crema (CR), Italy*

## Abstract

*High Dynamic Range (HDR) imaging techniques capture greater ranges of scene information, and attempt to convey that information with HDR displays. HDR imaging can improve the rendering of most scenes. Is the improved appearance caused by the increased luminance range and increased accuracy of display luminances? This paper examines the effect of increased luminance range on appearance in uniform color spaces. Our experiments show that increasing the luminance range of a transparent display by a factor of 500 has minimal effect on appearance. Two important image-dependent mechanisms are responsible for the small amount of change. First, intraocular scattered light, or veiling glare, limits the range of luminances on the retina. Second, human spatial processing, as seen in simultaneous contrast experiments, makes scatter limited retinal images appear to have higher contrast. These two image-dependent mechanisms work to counteract each other. Scatter acts to decreased the stimulus range on the retina, and spatial comparisons heighten apparent contrast. Both mechanisms are responsible for the observed small changes in the appearance range with large changes in luminance range.*

## Introduction

This paper studies the interrelationship of three aspects of Human Color Vision. In the 1860s, Maxwell made the first measurements of human color sensitivity[1]. Since then, color has been studied using psychophysics to measure color matches and color appearances. Since 1964, physiological measurements of cone receptors' absorption spectra and electrophysiology have studied color vision at the cellular level [2-4]. Since 1971, High Dynamic Range (HDR) image capture and image processing have studied color in the computer for processing and reproduction [5, 6]. Psychophysics, physiology and HDR imaging are three parts of today's color. However, they are often discussed independently without considering their inter-relationships. This paper studies the points of agreement, points of possible disagreement, and the framework of how to combine all three disciplines.

## Uniform color spaces – Psychophysics

Human psychophysical data has two distinct data sets describing color. The first set is Color Matching Functions (CMF), which describe when the two halves of a circle, each with a different spectral composition, will match [1]. Such color identities can be predicted by converting spectral radiance measurements (380 to 700 nm) into the tristimulus values X, Y, Z using the 1931 CIE standard CMF functions[7]. Since psychophysics has no technique for measuring the peak wavelength sensitivities of L, M, and S cones, X, Y, Z are attempts at measuring linear transforms of cone sensitivities convolved with pre-retinal absorptions. The XYZ color matching functions can be used to predict whether patches will match, but cannot predict color appearance of those patches, because X, Y, Z cannot take into account human spatial processing of other stimuli in the field of view [8].

The second distinct set of color data describes uniform color spaces. The X, Y, Z values, from color matching experiments, form a 3D space. X, Y, Z space is not isotropic in appearance. Euclidean distance between two different locations in X, Y, Z space does not predict equal changes in appearance. Munsell [9] and others [10-11] asked observers to find samples that appeared to be equally spaced.

A uniform color space is important in both theoretical and practical aspects of color theory and color applications. A uniform color space places observer data in an isotropic appearance 3D space. This information is critical in color theory because it provides the basis set for models of appearance [7, 12]. This information is critical in color reproduction because we can use it to distribute limited scene data (24 bit) so as to minimize quantization artifacts[13].

Munsell, Ostwald, OSA Uniform Color Space, NCS, and ColorCurve are examples of observations leading to uniform color spaces. Munsell is unique because it is has no external restrictions imposed on the observers [11].

ClELAB, CIELUV, CIECAM are examples of computational models of uniform color spaces. In this paper we use CIELAB. We realize that there are other more recent color space models and that there are issues of accuracy of uniformity associated with L*a*b* [11]. Nevertheless, L*a*b*, with its long history and great computational expediency, has great popularity and common usage. For these reasons, along with the fact that so many people are familiar with L*a*b*, we will use it to as the computational model that converts quanta catch by receptors into color appearance in this paper.

### *Conversion of radiance to calculated position in L* a* b* uniform color space*

CIE 1931 standard colorimetry calculates the tristimulus X, Y, and Z triplet from radiance, by integrating the light spectrum coming to the eye with the $\bar{x}, \bar{y}, \bar{z}$ color matching functions.

Using CIE1976 standard color space, we calculate L*a*b* from X, Y, Z [14]. Lightness (L*) calculates appearances between white and black; a* calculates appearances between red and green-blue; b* calculates appearances between yellow and blue. The goal of these formulae is to be able to convert X, Y, Z to an isotropic color space, where all constant Euclidean distances have constant differences in appearances.

The formulas for converting linear (radiance) spectral (XYZ) to L*a*b* are as follows:

$$L^* = 116\left(\frac{Y}{Y_n}\right)^{1/3} - 16 \qquad (1)$$

$$\text{If } \left(\frac{Y}{Y_n}\right) < 0.008856, \text{ then } \quad L^* = 903.3\left(\frac{Y}{Y_n}\right) \qquad (1a)$$

$$a^* = 500\left[\left(\frac{X}{X_n}\right)^{1/3} - \left(\frac{Y}{Y_n}\right)^{1/3}\right] \qquad (2)$$

$$b^* = 200\left[\left(\frac{Y}{Y_n}\right)^{1/3} - \left(\frac{Z}{Z_n}\right)^{1/3}\right] \qquad (3)$$

where $X_n$, $Y_n$, $Z_n$ are the integrals for the reference white (radiant power reflected from a perfect diffuser in the viewing illuminant). For equations 2 and 3, when any of the ratios $X/X_n$, $Y/Y_n$, $Z/Z_n$ is less, or equal to 0.008856, then:

$[(X/X_n)^{1/3}]$ is be replaced by $[7.787*(X/X_n)\ 16/116]$,
$[(Y/Y_n)^{1/3}]$ is be replaced by $[7.787*(Y/Y_n)+16/116]$,
$[(Z/Z_n)^{1/3}]$ is be replaced by $[7.787*(Z/Z_n)+16/116]$

The way that L*a*b* handles High Dynamic Range (HDR) scenes has two components. The first is the use of cube root functions in both lightness and chroma. The second is use of other functions to force the calculation to zero asymptotes.

In all cases, in evaluating this set of equations the first thing one does is to normalize the long-, middle- and short-wave integrals to the maxima in each channel; $(X/X_n)$, $(Y/Y_n)$, $(Z/Z_n)$. Human vision normalizes appearances to maxima in L, M and S channels[15-17]. This operation converts quanta catches to relative luminances.

The next step in all calculations raises these normalized integrals to the power of 1/3, or cube root. This exponential step shapes the normalized X, Y, and Z to approach color space uniformity. In HDR terminology, this step scales the large range of possible radiances into a limited range of appearances.

Figure 1 shows calculated Lightness L* (equations 1, 1a) vs. log luminance for a range covering six log units. Since we are concerned with the study of color over HDR images, we will plot luminance information as relative optical density ($OD=\log_{10}[1/(Y/Y_n)]$). The vertical yellow line identifies the luminance that divides the regions used. On the right side of the yellow line equation (1) applies; on the left side equation (1a) applies.

L* describes white as 100. On this graph L* = 100 plots at 0 relative optical density, or 100% $(Y/Y_n)$. When we reduces relative luminance by one half, then equation (1) reduce L* by 24%. In order to get L* = 50, we have to reduce luminance to 18%. The yellow line delimits the ranges of L* equations and falls at 9% in Lightness and 0.9% in luminance. There is no cube root function in equation 1a. It controls the shape of the asymptote to 0 lightness. L*=1 falls at OD = 3.0, or 0.1% luminance. In other words, L* suggests that 99% of usable $(Y/Y_n)$ information falls in 3 log units of scene dynamic range. Since a* and b* use the same compressive cube root function on $(Y/Y_n)$, $(X/X_n)$, $(Z/Z_n)$, then L* a* b* evaluates the very large range of X, Y and Z in the scene, over a 3 log unit cube. Uniform color spacing is achieved by the cube root function. The calculations a* and b* uses a different function below 0.9% relative luminance.

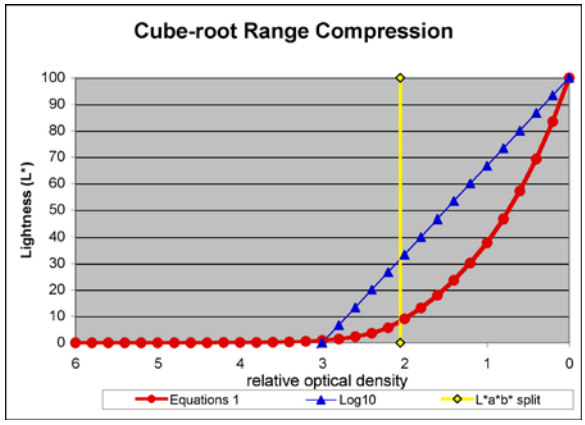


*Figure 1 plots Equation 1 and 1a (circles) vs. relative optical density. The yellow line delimits the range of each equation. L* reaches a value of 1 at OD = 3.0. For comparison, the triangles plot a log10 function over 3 log units.*

Figure 1 (triangles) plots a 3.0 log unit $\log_{10}$ function. By comparison, L* changes more quickly over the OD range 0.0 to 1.0, and more slowly over the OD range 1.0 to 3.0.

The study of psychophysics provides a description of human color vision. Since all data comes from asking observers to perform specific tasks, we can think of this as a top-down analysis of entire visual system.

## Color vision - Physiology

Although psychophysical measurements of human spectral sensitivities had a century-long head start, actual measurements of the absorption spectra of single rods and cones have been possible for 40 years. Marks Dobelle and Mac Nichols [2] and Brown and Wald [3], measured single cone cell spectral absorptions. About the same time, physiologists measured the electrical response of retinal summation cells to different levels of light. They reported that response to light was proportional to log luminance [4].

The study of physiology provides a second powerful description of human color vision. Since all data comes from biophysical measurements of single-cell preparations, we can think of this as a bottom-up analysis of light- and charge-responsive cells.

## Do psychophysics and physiology agree?

The top-down and bottom-up data do not agree. The actual peak sensitivities of cone pigments are very different from the assumed peaks in color matching functions. The single cell response to light is logarithmic, while psychophysics describes a cube-root function of Lightness vs. luminance. Are these serious discrepancies, or are these different results easily reconciled?

### *Spectral sensitivity*

The comparisons of spectral sensitivity of human cones, color matching functions, and camera spectral sensitivities have very interesting properties [18]. If one expects that cones respond the same as color matching functions, then one would be surprised at just how different these sensitivity functions are. The peak sensitivity of the cones are 440, 540, and 565 nm. [2,3] Dartnall, Bowmaker and Mollon [19] have shown similar results with peaks at somewhat shorter wavelengths. The peak sensitivities of XYZ are 450, 555, 610. The wavelength of CIE $\bar{x}$ peak sensitivity is 45 nm longer than the Lcone peak. The inclusion of pre-retinal absorptions helps somewhat to

reconcile these discrepancies. They shift the peak sensitivities to longer wavelengths.

Since the colorimetrists on the CIE 1931 Committee did not know the actual peak sensitivities of cones, they had to assume one of a very large set of possible linear transforms of matching data. Smith and Pokorny [20] argued that X, Y, Z are not inconsistent with actual cone sensitivities for color matching, as long as pre-retinal absorptions were included in the calculation.

### *Intensity response*

Werblin and Dowling [4] showed that single cell recording of summation responses of horizontal cells are proportional to log light intensity. There is no evidence of a cube root function in retinal response to light.

Stiehl et al. [21] studied images that contained equally spaced steps in lightness appearance. They measured the light coming from the display, *corneal luminance*, of these equally spaced lightness steps. Figure 2 plots Stiehl's 9-step Lightness data (tiangles), rescaled to 100 to 1. Their data falls on top of the CIELAB and CIELUV L*function (circles).

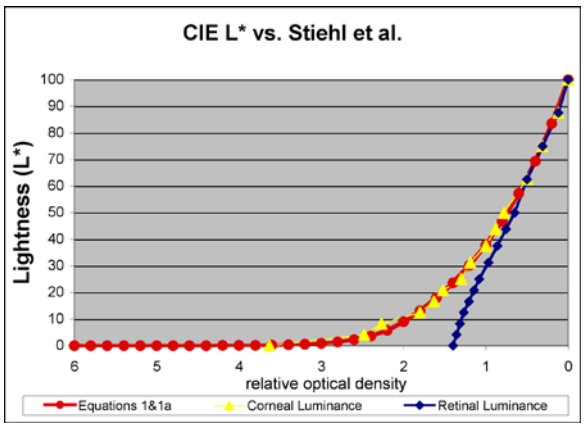


*Figure 2 plots Equation 1 and 1a (circles) vs. relative optical density. The yellow triangles plot the Stiehl et al. corneal luminance data for equal steps in lightness. The yellow triangles are measurements of target luminances made at the location of the observers' cornea. The diamonds are calculated luminances at the retina after intraocular scatter. Stiehl calculated a range of 1.4 log units on the retina for this target.*

Stiehl et al. [21] also used the point-spread function of the human eye to calculate the luminance on the retina after intraocular scatter. They found a different relationship between retinal luminance and appearance. Log *retinal luminance* is proportional to lightness appearance.

The cube-root function in CIE Lab and Luv derives from scattered light. Just as pre-retinal spectral absorptions are critical to reconciliation of physiological and psychophysical data, pre-retinal veiling glare is critical in reconciling equally spaced lightness scales with the physical stimulus. Figure 2 plots L* vs. Stiehl et al.'s retinal and corneal luminances in the same manner as Figure 1. Stiehl's calculated retinal luminance covers a much smaller range of luminances and shows the same linear response to log luminance reported by physiologists.

Measurements of both spectral sensitivity and lightness show the significant impact of intraocular modifications of the target stimulus by absorption and scatter.

## HDR imaging

When experimenters measure human response to light with single spots of light, they find a dynamic range of more than 10 log units for the combined responses of rods and cones However, the dynamic range of optic nerve cells is close to 2 log units.

Experiments with ordinary scenes show that the white to black range of appearances have dynamic ranges of luminance between 2 to 4 log units [22-27]. There are two important reasons for appearance to be different for real scenes, than for small spots of light. The first is an optical mechanism, associated with the effect of intraocular scattered light, or glare [28-30]. The second is a physiological mechanism, associated with the effect of spatial interactions in the human visual system [26]. Both the optical and physiological spatial processes play a major role in determining the appearance of areas in an image.

### *Image acquisition*

Glare is the scene- and camera-dependent scattered light falling on image sensors. First, glare limits the range of luminances that can be accurately measured by a camera, despite multiple exposure techniques. McCann and Rizzi [26, 27] used 4.3 log dynamic range test targets and a variety of digital and film cameras. In each case, the camera response to constant luminances varied considerably with changes in the surrounding pixels. HDR image capture cannot accurately record the luminances in these targets. The improvement in HDR images, compared to conventional photography, does not correlate with accurate luminance capture and display. Accurate capture is not possible, and accurate rendition is not essential. The improvement in HDR images is due to better preservation of relative spatial information that comes from improved digital quantization. Spatial differences in highlights and shadows are not lost [26, 27].

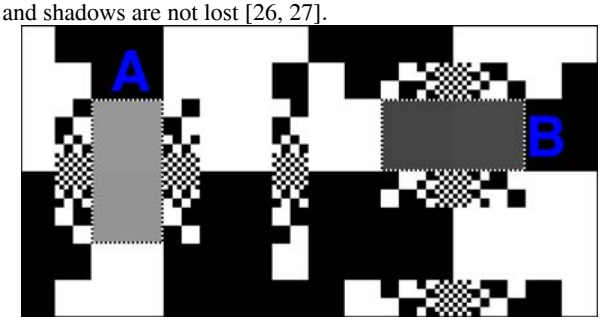


***Figure 3*** *Magnified view of two of twenty gray pairs of luminance patches. The left half (square A) has the same layout as the right (square B), rotated 90° counterclockwise. The gray areas in A have slightly different luminances, top and bottom. The gray areas in B have different luminances, left and right. The square surrounding areas are identical except for rotation. For each size there are equal numbers of min and max blocks.*

### *Human Observation*

We measured the appearance of grays in test targets with different ranges of luminances. The dynamic range of a single transparency was 500:1, or 2.7 log units. The surround area was 50% maximum transmission and 50% minimum transmission. We wanted a surround that is, on average, equal to the middle of the dynamic range. To approximate real images we distributed the half-white half-black areas in different size squares. In this way, we have energy over a wide range of spatial frequencies, similar to real scenes, and can avoid the problem that simultaneous contrast depends on the size of the adjacent white areas [31, 32].

Figures 3 and 4 shows the layout of our min/max test target. The display subtended 15.5 by 19.1 degrees. It was divided into 20 squares, 3.4 degrees on a side. Two 0.8 degree gray patches are within each square along with various sizes of max and min blocks. The two gray-square length subtends an angle approximately the diameter of the fovea. The smallest block (surrounding the gray patches) subtends 1.6 minutes of arc and is clearly visible to observers. We used 2x, 4x, 8x, 16x, 32x, 64x blocks around each gray pair.

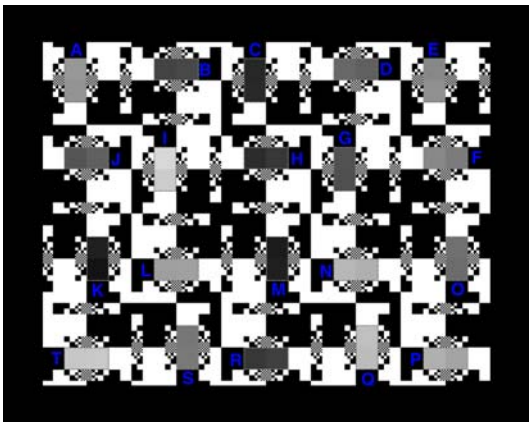


***Figure 4*** *Target with twenty gray pairs of luminance patches. All gray pairs are close in luminance, but some edge ratios are larger than others.*

The second experiment added a second, identical transparency in superposition to the first. This doubled the optical densities of the target. The display dynamic range changed from 2.7 to 5.4 log units O.D. The contrast of the image remained the same: 50% of the area was maximum transmission and 50% was minimum transmission. The black optical density doubled. However the 50% white surround is by far the major contributor to scattered light. Doubling the density of each area in the target will have minimal effect on the image's scattered light [33].

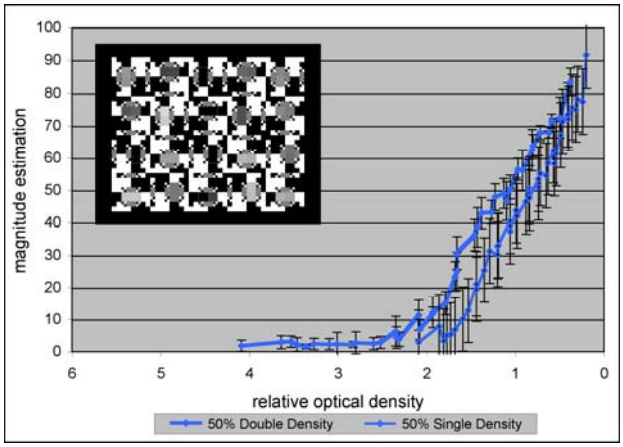


***Figure 5*** *Appearances of single- (SD) and double-density (DD) displays with 50% average luminance surround. Observers estimate the same range limit of 2.3 log units.*

In these experiments, we asked observers to use magnitude estimates between the appearance White (MagEst=100) and Black (MagEst=1). Five observers made 5 estimates of 40 gray squares in a transparent target on a lightbox. The plot of magnitude estimate vs. relative optical density for this single density target is shown in Figure 5(line on the right).

The plots for single- and double-density nearly superimpose. The curves show the same asymptote at white and black. At middle gray (MagEst=50), the single-density curve is about 0.24 OD higher luminance (Figure 5). When simultaneous contrast and scatter are held nearly constant, the plots of appearance are nearly constant, despite dramatic increases of dynamic range. In other words, doubling the dynamic range of this target causes only minimal changes in appearance. Increases of target dynamic range by 2.7 log units are unusable, and invisible, in this background.

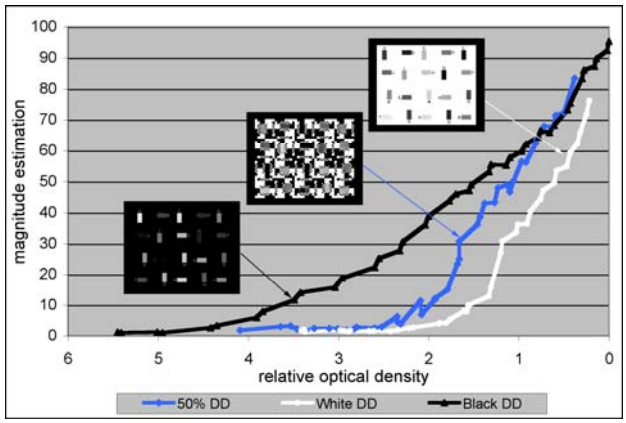


***Figure 6*** *Appearances of double-density (DD) displays with 100%, 50% and 0% white backgrounds. Observers' magnitude estimates show that 2.0, 2.3 and 5.0 log units of scene, or corneal luminance, are usable.*

Further experiments that change the surround show similar results. These experiments used 100% white and 0% white background. The analysis of these results [33] shows the substantial effects of intraocular scatter. The luminance on the retina plays a major role controlling appearance. The combined effect of glare and simultaneous contrast correlates with appearance.

### *Intraocular Scatter and Lightness*

Rizzi et al. [34] calculated the retinal luminance for the targets in Figure 6. We started with the array of all scene luminances. We selected a pixel on the edge between two similar grays. We calculated the veiling glare contribution from all other pixels using the standard CIE Glare Spread Function [29]. We added glare to the pixel's luminance to obtain relative retinal optical density. We perform this calculation for displays with 100% white, 50% white and 0% white backgrounds. Plots of appearance vs. log scene luminance show three different, surround dependent, non-linear functions. Figure 7 plots of appearance vs. log retinal luminance show three different, surround dependent, linear functions. Figure 7 also plots the Stiehl et al. calculated retinal luminance described in Figure 2. Stiehl's target and Rizzi's 100% white target share the same function of relating Lightness to retinal luminance. Increasing the amount of white in the background decreases the dynamic range of the retinal image because of glare. Increasing the amount of white in the background increases the apparent contrast of the image. Glare and physiological spatial contrast act in opposition to each other. They tend to cancel each other.

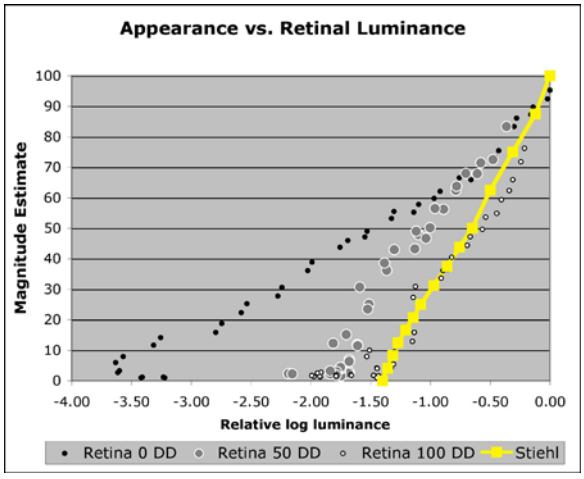


*Figure 7 plots calculated retinal luminance vs. relative optical density for four different targets. The black dots plot Rizzi's 0% white; the gray circles plot Rizzi's 50% white background target; and the white dots plot Rizzi's 100% white background targets. The yellow triangles plot Stiehl et al. data for equal steps in lightness.*

We fit the MagEst data with a logarithmic function with variable slopes:

$$\text{MagEst} = 100 - \mathbf{m}[\log 10(1/(Y/Y_n))], \quad (4)$$
$$\text{MagEst} = 100 - \mathbf{m}[\text{relative optical density}],$$

where **m**=71.4 for 100% white; **m**=50 for 50% white, and **m**=27 for 0% white surround (Figure 8). The equation multiplies the scene dependent slope **m** by the pixels optical density.

The range of slope **m**, and the strength of the spatial processing is much greater than one might expect for observations of everyday life. The reason is that these spatial processes work in opposition to intraocular scatter. The two tend to cancel, helping to achieve appearance constancy. The slope of these lines is controlled by spatial interactions responsible for simultaneous contrast phenomena.

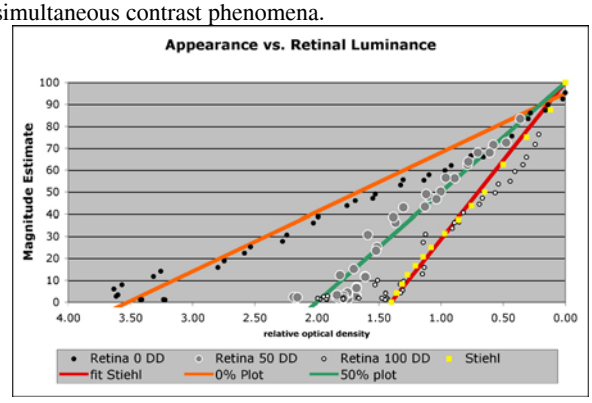


*Figure 8 plots calculated retinal luminance vs. relative optical density for four different targets along with fits to MagEst with equation (4).*

## Discussion

The data in Table 1 show that intraocular scatter reduces the range of the displays' *corneal luminances* to much smaller range of *retinal luminances*. The effect of scatter is scene dependent.

| %White | Stiehl, et al. | 100%white | 50%white | 0%white |
|---|---|---|---|---|
| Target | 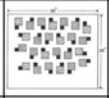 | 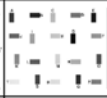 |  | 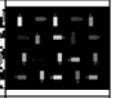 |
| Usable Range (OD) MagEst (100 to 1) | | 2.0 | 2.3 | 5.0 |
| Range (OD) at cornea | opaque blacks | 5.3 | 5.4 | 5.8 |
| Range (OD) at retina | 1.4 | 1.4 | 2.0 | 3.5 |
| slope **m** | 71.4 | 71.4 | 50 | 27 |

***Table 1** summarizes the results. The top row lists the target names. The second row shows the experimental displays. The third row lists the usable range of luminances observers selected to cover appearances from MagEst=100 to MagEst=1(from Figure 6). The fourth and fifth rows list the range of luminances measured at the cornea (from calibration) and calculated at the retina (from Figure 7). The bottom row lists the slope **m** used in equation (4) to fit the retinal luminance vs. MagEst (Figure 8).*

Scatter, by its very nature, affects lower luminances more than higher ones. In order to study the spatial properties of vision one must analyze retinal luminances. Figure 7 shows that all targets analyzed (uniform surrounds) showed that lightness correlates with the function of log luminance. The slope **m** is scene dependent. Figure 8 data shows that the values of **m** variy by a ratio of **2.6:1**. The effect of scattered light reduces the contrast of the display, and decreases the slope of appearance vs. luminances. Spatial processing counteracts scatter by increasing the slope of appearance vs. luminance. It not only cancels scatter, but overcompensates, leaving the examples of simultaneous contrast as the residual. A gray paper in a white surround is only 10% darker than the same gray on black. Equal retinal stimuli must show larger changes in appearance. In other words, veiling glare masks the powerful spatial processing in vision. This spatial processing would be more dramatic without the influence of veiling glare. Regardless, spatial processing acts to minimize the effect of glare. Since both glare and spatial processing are complex, scene-dependent processes with different spatial properties, they do not exactly cancel. Rather, the spatial physiology reduces the effect of glare and contributes to the constancy of vision. To understand these phenomena in detail, we must study each process's complex spatial response to the entire scene.

## Conclusions

Intraocular glare, or scattered light, controls the dynamic range of luminances falling on the retina. Simultaneous contrast, a physiological spatial mechanism, generates appearances by comparing different parts of the image.

This paper reports experiments using high-dynamic range test targets. These experiments show that the dynamic range of appearance is image content dependent, not luminance range dependent. Our experiments measured the appearance of grays in single- and double-density displays with the same spatial patterns. We compared the change in appearance of all grays

with change in both corneal and retinal luminances. Whereas corneal luminance measures a cube-root response function, retinal luminance measures a logarithmic response function. Intraocular scattered light explains the cube root central to Lab and Luv color spaces. The change of appearance of grays on a uniform lightness scale is image dependent. It depends on both the intraocular scatter and the spatial processing of each scene.

## Acknowledgements

The authors wish to thank Marzia Pezzetti for he work performing these measurements. We also want to thank Ivar Farup and Mary McCann for their help and discussions.

## References

[1] W. D. Niven, ed., The Scientific Papers of James Clerk Maxwell, (Dover Publications, Inc., New York, 1965) 410–444.

[2] W. B. Marks, W. H. Dobelle, & E. F. MacNickol, Visual pigments of single primate cones, Science **143**, 1181, (1964).

[3] P. K. Brown & G. Wald, "Visual pigments in single rods and cones of the human retina of human retina", Science **144**, 45, (1964).

[4] F. S. Werblin and J. E. Dowling, "Organization of the Retina of the Mudpuppy, *Necturus maculosus*. II. Intracellular Recording", J. Neurophysiol. 32, pp. 339-355, (1969).

[5] E. Land and J. J. McCann, "Lightness and Retinex Theory", J. Opt. Soc. Am., 61, pp. 1-11, 1971

[6] J. Frankle and J. J. McCann, "Method and apparatus of lightness imaging", U. S Patent 4,384,336, submitted (1983).

[7] CIE Proceedings 1931, p. 19, Cambridge University Press, Cambridge, (1932).

[8] G. Wyszecki, "Colorimetry" in Color Theory and Imaging Systems, Society of Photographic Scientists and Engineers, R. Eynard, ed., Washington, p. 38, (1973).

[9] A. E. O. Munsell, l. l. Sloan and I. H. Godlove, "Neutral Value Scales, I. Munsell neutral scale, J. opt Soc. Am, 23 394, (1933).

[10] .S. M. Newhall, D. Nickerson. and D. B. Judd, "Final report of the OSA. Subcommittee on spacing of the Munsell colors", J. Opt. Soc. Am. 33, 385 (1943).

[11] J. J. McCann, "Color spaces for color mapping", J. Electronic Imaging, **8**, 354-364, (1999).

[12] M. D. Fairchild. Color Appearance Models, (Addison Wesley, Reading, MA, 1998).

[13] M. Abdulwahab, J. L. Burkhardt, and J. J. McCann, "Method and apparatus for transforming color image data on the basis of an isotropic colorimetric space: ' U.S. Patent. No. 4,839,721 (filed June 13, 1989).

[14] CIE, "Recommendation on Uniform Color Spaces, Color Difference Equations, Psychometric Color Terms", Supplement No 2 of CIE Publ. No. 15 (E-1.3.1) 1971, Bureau Central de la Paris, (1978).

[15] E. H. Land, The Retinex, *Am. Scientist,* 52, pp. 247-264, (1964).

[16] J. J. McCann S. McKee and T. Taylor, Quantitative studies in Retinex theory: A comparison between theoretical predictions and observer responses to 'Color Mondrian' experiments" Vision Res. **16,** 445-458, (1976).

[17] J.J. McCann, Rules for Colour Constancy, *Opthal.Opt.,* 12, pp 175-177, (1992).

[18] J. J. McCann, "The history of spectral sensitivity functions for humans and imagers: 1861 to 2004", in Color Imaging X: Processing, Hardcopy, and Applications, Proc. SPIE, Bellingham, WA, 5667, pp. 1-9, (2005).

[19] H. J. A. Dartnall, J. K. Bowmaker, & J. D. Mollon, "Human visual pigments: microspectrophotometric results from the eyes of seven persons", Proceedings of the Royal Society of London, **B 220**, 115-130, (1983).

[20] V. C. Smith and J. Pokorny, "Spectral Sensitivity of the Foveal Cone Photopigments between 400 and 500 nm," Vision Res., 15, p. 161, (1975).

[21] W. A. Stiehl, J. J. McCann & R. L. Savoy, "Influence of intraocular scattered light on lightness-scaling experiments", J. Opt. Soc. Am., 73, pp. 1143-1148, (1983).

[22] J. J. McCann and A. Rizzi, "Optical veiling glare limitations to in-camera scene radiance measurements", in ECVP 2006 Abstracts, Perception, Vol. 35. Supplement, p. 51, 2006.

[23] J. J. McCann and A. Rizzi, "Spatial Comparisons: The Antidote to Veiling Glare Limitations in HDR Images", in Proc ADEAC/SID&VESA, Atlanta, 155-158, 2006

[24] J. J. McCann and A. Rizzi, "Veiling glare: the dynamic range limit of HDR images", in Human Vision and Electronic Imaging XII, eds. B. Rogowitz, T. Pappas, S. Daly, Proc. SPIE, Bellingham WA, , 2007, 6492-41, 2007.

[25] J. J. McCann and A. Rizzi, "Spatial Comparisons: The Antidote to Veiling Glare Limitations in Image Capture and Display" in IMQA2007 The Second Int. Workshop on Image Media Quality and its Applications, Chiba, Japan, E-1, 2007

[26] J. J. McCann, "Art, science, and appearance in HDR images", J Soc Info Display 15/9, 709-719 (2007).

[27] J. J. McCann and A Rizzi, "Camera and visual veiling glare in HDR images," J Soc Info Display 15/9, 721–730 (2007).

[28] ISO 9358:1994 Standard, "Optics and optical instruments. Veiling glare of image forming systems. Definitions and methods of measurement", (ISO, 1994).

[29] Vos, J.J. and van den Berg, T.J.T.P [CIE Research note 135/1, "Disability Glare"] ISBN 3 900 734 97 6 (1999).

[30] CIE 146/147:2002, CIE Collection on Glare 2002, Commission Internationale de L'Eclairage, (2002).

[31] J. J. McCann, "Visibility of gradients and low-spatial frequency sinusoids: Evidence for a distance constancy mechanism", J. Photogr. Sci.Eng., 22, 64-68, (1978).

[32] J. J. McCann and A. Rizzi, "The Spatial Properties of Contrast', in Proc. IS&T/SID Color Imaging Conference, Scottsdale; 11, p. 51-58, (2003).

[33] A. Rizzi, M. Pezzetti, J.J. McCann, Glare-limited Appearances in HDR Images, IS&T/SID *Color Imaging Conference 2007,* Albuquerque (New Mexico), November , 2007.

[34] A. Rizzi, M. Pezzetti, and J. .J. McCann, "Separating the Effects of Glare from Simultaneous Contrast", in Human Vision and Electronic Imaging XIII, Proc. SPIE, Bellingham, WA, 6806-09 (2008).

## Author Biography

*John McCann (1964 AB. Degree, Biology, Harvard) worked in and managed, the Vision Research Laboratory, Polaroid(1961-1996). His 120 publications have studied Retinex theory, rod/Lcone color interactions at low light levels, appearance with scattered light, and HDR imaging. He is a Fellow IS&T, OSA; past President IS&T, Artists Foundation, Boston. He continues his research on color vision. He received the SID Certificate of Commendation, IS&T/OSA 2002 Edwin H. Land Medal, IS&T Honorary Member.*

*Alessandro Rizzi took degree in Computer Science at University of Milano and PhD in Information Engineering at University of Brescia. Now he is assistant professor, and senior research fellow at the Department of Information Technologies at University of Milano. Since 1990 he is researching in the field of digital imaging and vision. His main research topic is color information with particular attention to color perception mechanisms. He is the coordinator of the Italian Color Group.*

 